

Water Bamboo Husk-Reinforced Poly(butylene succinate) Biodegradable Composites

Yeng-Fong Shih,¹ Wan-Chien Lee,² Ru-Jong Jeng,² Chien-Ming Huang¹

¹Department of Biochemical Engineering, Hsiuping Institute of Technology, Taichung, 412, Taiwan, Republic of China

²Department of Chemical Engineering, National Chung Hsing University, Taichung, 402, Taiwan, Republic of China

Received 9 March 2005; accepted 8 May 2005

DOI 10.1002/app.22220

Published online in Wiley InterScience (www.interscience.wiley.com).

ABSTRACT: The water bamboo husk is one of major agricultural wastes in Taiwan. In this study, the fiber and powder obtained from the water bamboo husk were chemically modified by coupling agents. Furthermore, the modified fiber and powder were added to the biodegradable polymer poly(butylene succinate) (PBS) separately, to form novel fiber-reinforced composites. Morphologies, mechanical properties, and heat resistance of these water bamboo husk-reinforced composites were investigated. The results indicate that the fibers modified by coupling agents exhibited better compatibility with the polymer matrixes than did the untreated fibers. Moreover, it is found that the thermal properties were improved as plant fiber was incorporated to those polymers. Furthermore, the mechanical properties

were also increased with the addition of coupling agent-treated fiber. On the other hand, it is found that the homogeneity of untreated powder-containing samples is better than that of untreated fiber-containing samples. Moreover, the results reveal that the powders modified with coupling agents were not effective in improving the mechanical properties of the reinforced PBS. This is due to the bulky structure of lignin leading to a smaller reaction ratio with the coupling agents. © 2005 Wiley Periodicals, Inc. *J Appl Polym Sci* 99: 188–199, 2006

Key words: water bamboo; fiber; biodegradable polymer; PBS

INTRODUCTION

Water bamboo (*Coba*, *Gau sun*) is a water plant that has a preference for warm, humid, and sunny environment. The peak production is during summer.¹ Despite that water bamboo is a highly popular vegetable, the water bamboo husk is one of the major agricultural wastes in Taiwan. Recently, plant-based lignocellulosic fibers have attracted a great deal of interests for reinforcing plastics.^{2–20} The addition of plant-based lignocellulosic fibers to reinforce plastics not only served the purpose of reducing the amount of agricultural wastes, but also increased the biodegradation rate of plastics as well. Various researchers investigated the strengthening effects of the plant fibers containing polyolefins, polystyrene, polyester, polyurethane, and epoxy resins.^{2–15} Moreover, the plant fibers were further incorporated into biodegradable polymers (Master-Bi® and poly(butylene succinate)).^{16–20} Mechanical properties and biodegradability of the plant fiber-containing biodegradable polymers were greatly enhanced as compared with the

pristine biodegradable polymers. In this study, the fiber obtained from water bamboo husk was chemically modified by coupling agents to improve the compatibility with the plastics. Subsequently, the treated fiber was incorporated into a biodegradable polymer to enhance the mechanical and thermal properties of the plastics.

The biodegradable polymer used in this study is poly(butylene succinate) (PBS). PBS is synthesized through the polycondensation reaction of glycols such as ethylene glycol and 1,4-butanediol, and aliphatic dicarboxylic acids such as succinic acid and adipic acid. PBS is a white crystalline thermoplastic, has melting points similar to LDPE, glass transition temperatures and tensile strength in the range of that of PE and PP, stiffness in the range of that of LDPE and HDPE. PBS is a biodegradable polymer with strength and toughness, which are close to those of LDPE.²¹ This biodegradable polymer is considered highly promising as a commercial commodity polymer.

EXPERIMENTAL

Materials

The husk of water bamboo grown in Nantou County, Taiwan was chopped and screened between 40 mesh (0.3698 mm) and 80 mesh (0.175 mm) to obtain the fiber (F), and screened from 80 mesh (0.175 mm) to

Correspondence to: Y.-F. Shih (syf@mail.hit.edu.tw).

Contract grant sponsor: National Science Council; contract grant number: NSC 92-2216-E-164-001.

TABLE I
Formulations of Samples (wt %)

	Bionelle	Untreated powder	Untreated fiber	Powder treated by coupling agent	Fiber treated by coupling agent
B	100				
P		100			
F			100		
FZ6020					100 (Z6020)
FZ6040					100 (Z6040)
BP10	100	10			
BF10	100		10		
BP10Z6020	100			10 (Z6020)	
BP10Z6040	100			10 (Z6040)	
BF10Z6020	100				10 (Z6020)
BF10Z6040	100				10 (Z6040)

obtain the powder (P). The fiber and powder were then treated by silane coupling agents separately. The coupling agents (Z6020 and Z6040) were supplied by DecuChem Co. Ltd., Taiwan. Surface treatments of dried fiber and powder were carried out in the acetone solution of silane. Filler (5 g) and silane (0.5 g) were put in a flask with the proper volume of acetone. After agitation for 30 min, the flask was sealed with a polytetrafluoroethylene film and then kept at room temperature for 12 h. Then the samples were washed with acetone to remove compounds not covalently bonded to the fiber or powder, and then dried at 80°C in an oven to maintain constant weight. The poly(butylene succinate) (PBS, Bionolle #1001) was supplied by Showa Highpolymer Co. Ltd. Japan. The formulations of the samples were shown in Table I.

Preparation of the composites

The PBS, water bamboo fiber, and powder were dried in an air oven at 100°C for 4 h, until the moisture content reaches below 1.0 wt %. Then they were mixed in a plasticating extruder (a twin screw extruder of corotating type, with L/D = 43.5, and a low shear rate configuration) with barrel temperature ranging from 110 to 180°C. Extruded material was cut into small pellets in a granulator. Dumb-bell shaped specimens were obtained using a Battenfeld, Ba750 CDPLUS injection-molding machine with a mold temperature of 160–190°C.

Instruments

The elemental analysis was carried out on a Vario EL CHNOS analyzer produced by Germanic Elementar Company.

The composition of chemically modified fiber was analyzed by the X-ray photoelectron spectroscope (XPS, VG ESCA, England) with the scientific theta

probe. The X-ray source is Al K α (1486.6 eV) and X-ray spot size is 15–400 μ m.

The infrared spectra were obtained by a FTIR spectrometer (PerkinElmer Paragon 500) with a resolution 2 cm^{-1} by scanning 50 times from 300 to 4000 cm^{-1} at room temperature. All film samples were analyzed with the conventional NaCl disk method. The morphology of the fractured surfaces of samples was analyzed by SEM (TOPCON ABT-150S).

TGA analyses were conducted using a Seiko Instrument's TG/DTA220. All experiments were carried out under a nitrogen atmosphere at a purge rate of 100 mL/min. Samples of approximately 5 mg were heated to 600°C at a heating rate of 10°C/min.

Mechanical properties of samples were investigated using a PerkinElmer DMA 7e dynamic mechanical analyser (DMA) at frequency 1 Hz (heating rate of 3°C/min). The specimen size was 0.5 \times 0.5 \times 0.3 cm^3 .

Values of heat of combustion (HOC) of materials were determined by IKA[®]-WERKE C4000 adiabatic calorimeter (ASTM 240D) with a sample weight about 0.5 g. To confirm the complete removal of solvents and humidity, the sample was dried at 60°C until the constant weight was obtained. Benzoic acid was used for calibration of the calorimeter; its massic energy of combustion is $-(26,454 \pm 11) \text{ J g}^{-1}$ under certified condition. The bomb was made of stainless steel. The sample was put into a crucible inside the bomb. The oxygen pressure in the bomb was 3.04 MPa.

TABLE II
The Results of Elemental Analysis

	N (%)	C (%)	H (%)	O (%)	O/C
F	0.52	40.35	6.60	46.20	1.145
FZ6020	3.34	38.75	6.65	40.27	1.039
FZ6040	0.88	39.71	6.49	44.34	1.117

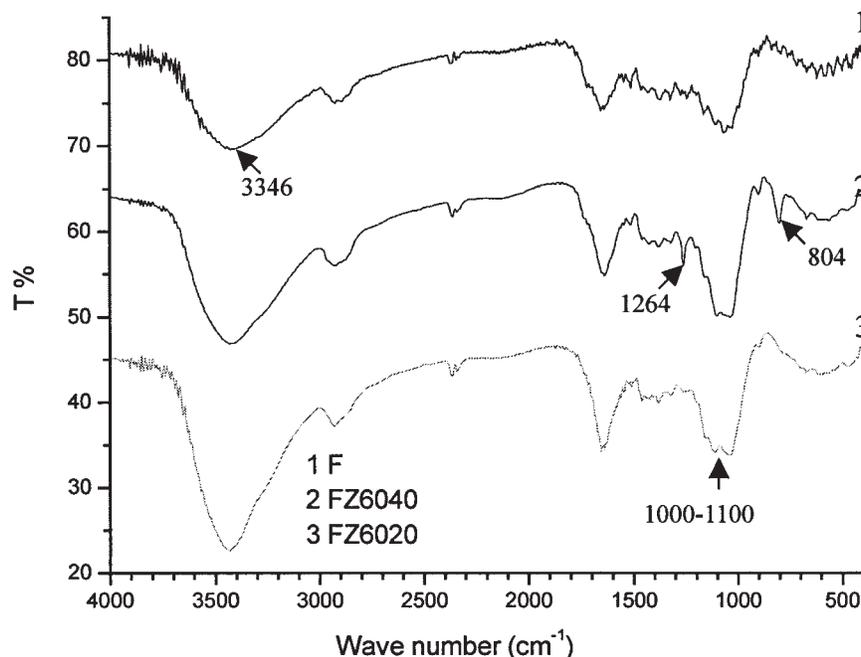


Figure 1 FTIR analysis for untreated and silane-treated fibers.

RESULTS AND DISCUSSION

Elemental analysis

The elemental analyses of untreated and treated fibers are shown in Table II. It is found that the content of nitrogen in FZ6020 fiber (fiber treated by coupling agent Z6020) is the largest. This is due to the amine groups present in the structure of Z6020. Moreover, it is important to note that the O/C ratios were decreased as the fiber is treated by coupling agent. The O/C ratios of FZ6020 and FZ6040 (fibers treated by coupling agent Z6040) were 1.039 and 1.117, respectively, which were smaller than that of untreated fiber (1.145). In fact, the O/C ratios of fiber (1.15), coupling agents Z6020 (0.5) and Z6040 (0.74) can be calculated by their chemical structure. The smaller O/C ratios of Z6020 and Z6040 are attributed to the methylene groups of the coupling agents, indicating the higher carbon content.²² Moreover, the decreased O/C ratios of fiber treated with coupling agents imply the chemical attachment of coupling agent on the fibers.

FTIR spectrum

As shown on Figure 1, a strong and broad absorption was found at 3346cm^{-1} . This implies the presence of —OH groups in the fiber. Furthermore, the hydrogen bonding between those —OH groups was present. After being treated by coupling agents, the absorption peak of —OH group in the fiber was shifted to higher wave number near 3400cm^{-1} . This implies that the degree of hydrogen bonding between —OH groups

has decreased, and the absorption peak of —OH groups has shifted to the position of free —OH groups (higher wave number).^{23,24} Furthermore, the peaks at 804 and 1264cm^{-1} were found for FZ6040. These are the characteristic absorption peaks of epoxide resulting from the coupling agent, Z6040. It is important that a slight increment in the broad peak around $1000\text{--}1100\text{cm}^{-1}$ is noted in all coupling agent-treated fibers. This could be attributed to the presence of the asymmetric stretching of —Si—O—Si— and/or to the —Si—O—C— bonds.^{25,26} The former bond is indicative of the existence of polysiloxanes deposited on the fiber and the latter would confirm the occurrence of a condensation reaction between the silane coupling agent and the fiber.

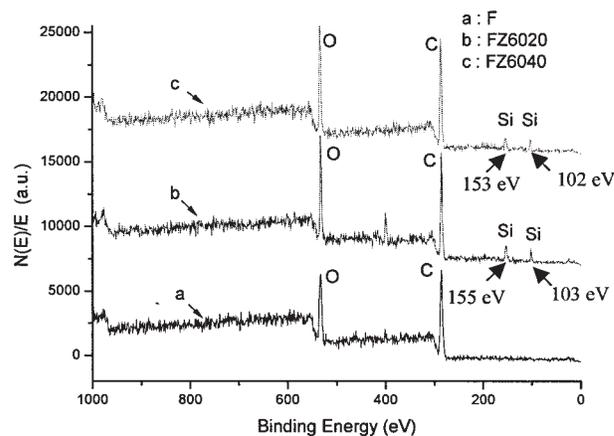


Figure 2 XPS survey spectra for untreated and silane-treated fibers.

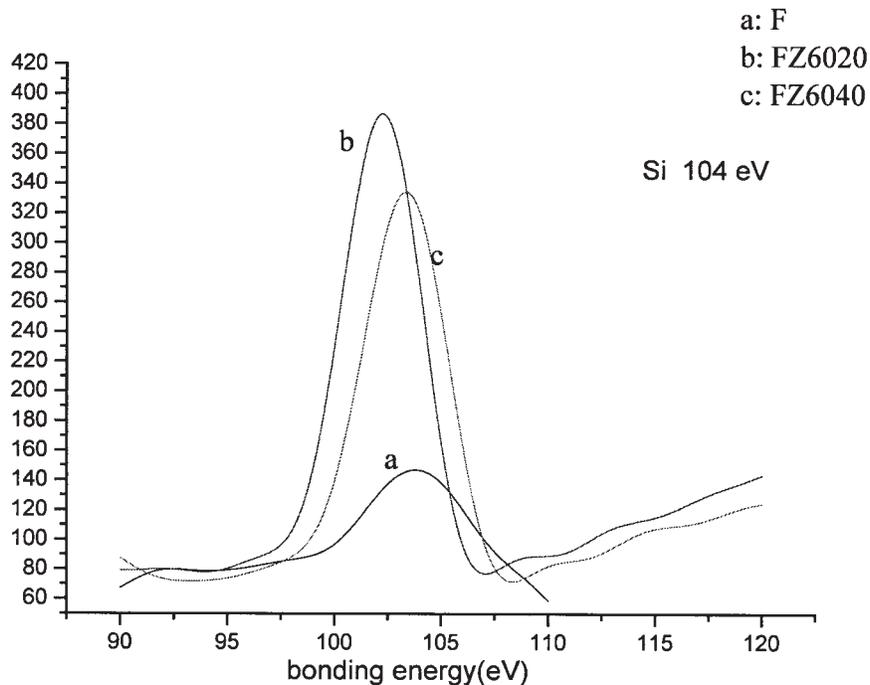


Figure 3 XPS spectra of silicon peaks (Si_{2p}) for untreated and silane-treated fibers.

XPS analysis

X-ray photoelectron spectroscopy (XPS) can provide information about surface composition and the chemical environment and bonding of surface chemical species.

The X-ray photoelectron spectroscopy shows the electron intensity as a function of the binding energy for the untreated and silane-treated fibers (Fig. 2). As

expected, for a lignocellulosic material, C_{1s} and O_{1s} are the predominant species and appear at 533 and 285 eV, respectively.²⁷⁻²⁹ In the case of the silane-treated fibers (FZ6020 and FZ6040), the presence of silicon on the surface of the fibers was detected from its characteristic emission peaks at about 150 and 100 eV, for Si_{2s} and Si_{2p} , respectively. Moreover, the peak area of Si_{2p} was obviously increased by the addition of silane cou-

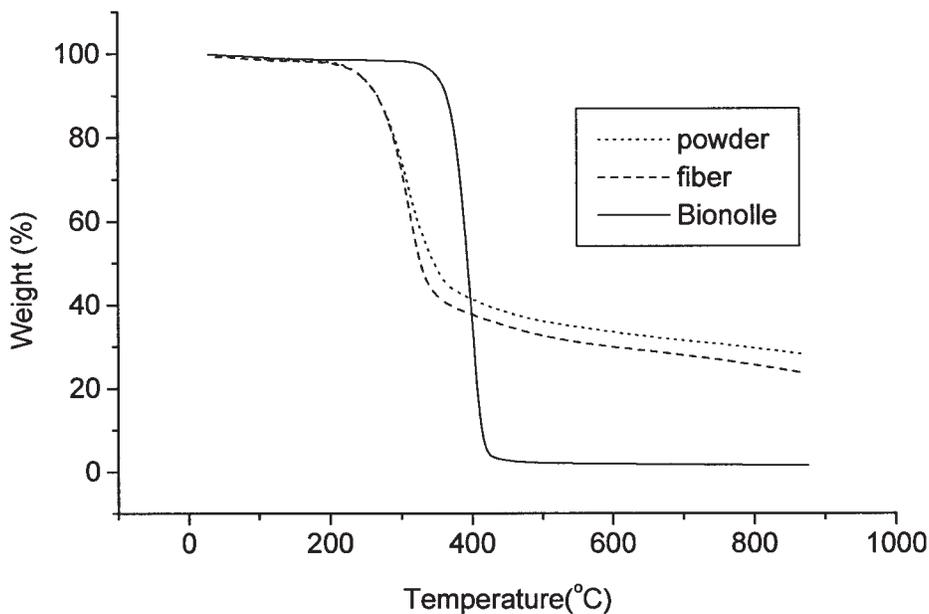


Figure 4 TGA thermograms of raw materials.

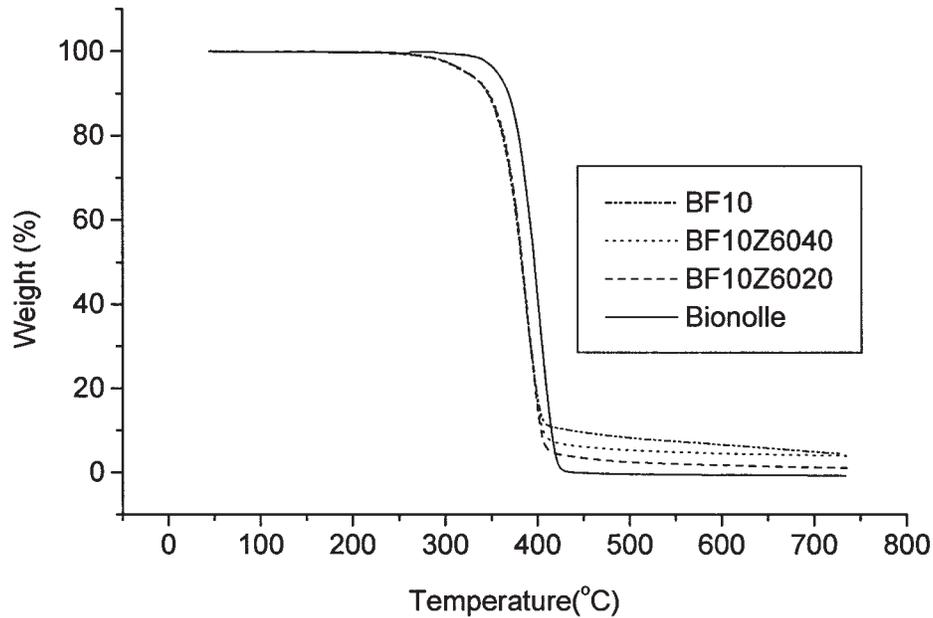


Figure 5 TGA thermograms of fiber-reinforced Bionolle composites.

pling agent as shown in Figure 3. This implies that the silicon content of the fiber was increased. Furthermore, the bonding energies of FZ6020 and FZ6040 in XPS are all larger than 102 eV. According to the literature,^{27,29} the apparition of emission peaks at binding energies greater than 102 eV reflects the bonding of the silicon atom with more than two oxygen atoms. These findings seem to confirm the presence of the silane group deposited on the surfaces of both FZ6020 and FZ6040 fibers. This indicates that the chemical

reaction between the hydrolyzed silane and the fibers has taken place.

TGA analysis

TGA thermograms of various samples under nitrogen are shown in Figures 4, 5 and 6, respectively. Figure 4 reveals that char yields (700°C) of Bionolle, powder, and fiber are 0, 32, and 28%, respectively. Obviously, the char yields of water bamboo powder and fiber

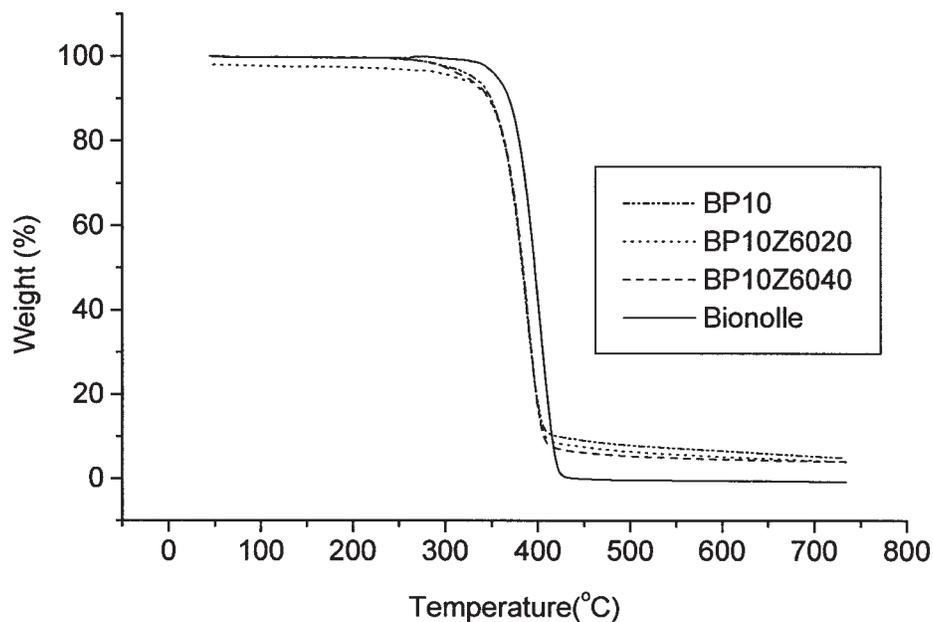


Figure 6 TGA thermograms of powder-reinforced Bionolle composites.



Figure 7 SEM photograph of Bionolle.

were larger than that of Bionolle. Moreover, the char yields of fiber-containing samples (BF10, BF10Z6040, and BF10Z6020) and powder-containing samples (BP10, BP10Z6040, and BP10Z6020) are all larger than that of Bionolle (Figs. 5 and 6). These results reveal that the addition of powder or fiber to Bionolle would

effectively raise the char yields of the samples. As reported previously,³⁰⁻³⁶ the char yield is directly correlated to the potency of flame retardation of the polymers. Increasing char formation can limit the production of combustible gases, decrease the exothermicity of the pyrolysis reaction, and inhibit the thermal con-

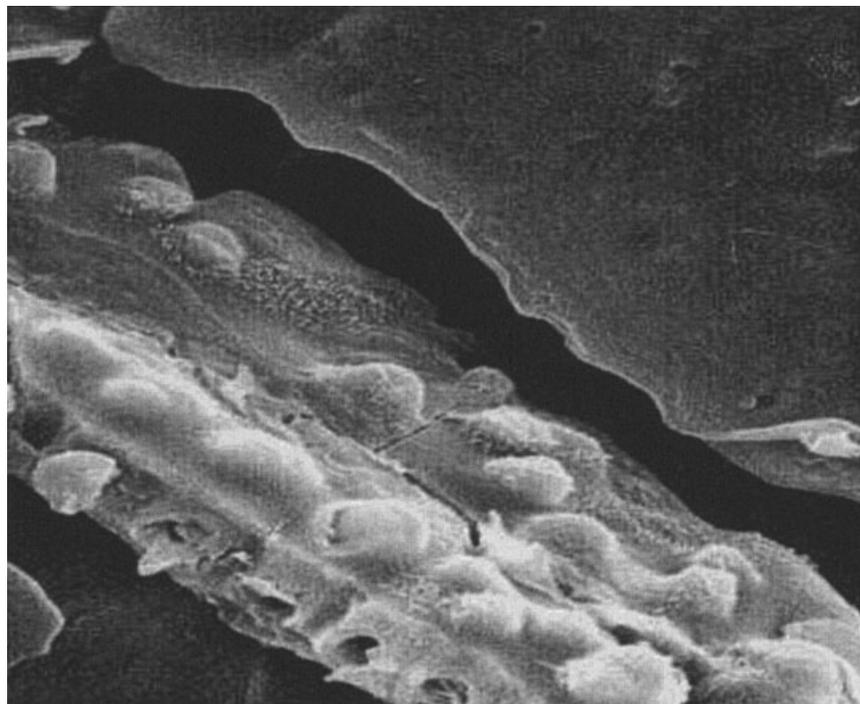


Figure 8 SEM photograph (2000 \times) of BF10.

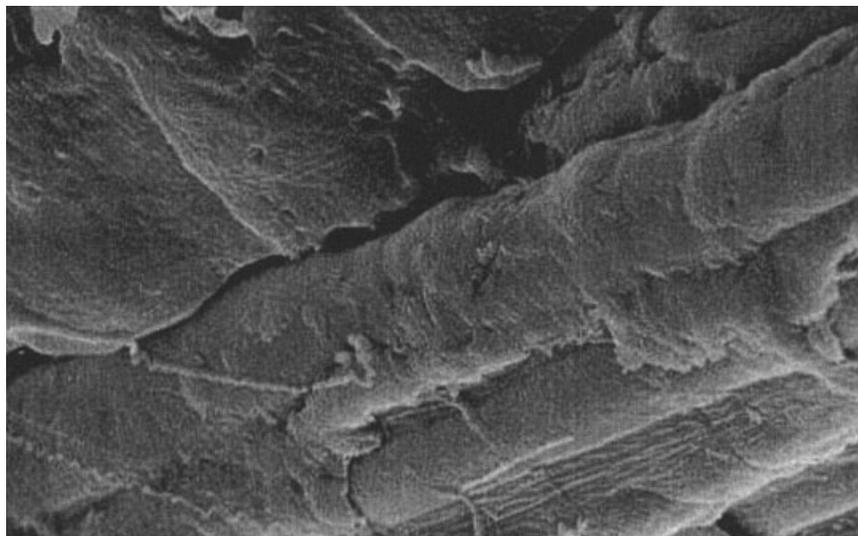


Figure 9 SEM photograph (2000 \times) of BF10Z6020.

ductivity of the burning materials.³⁷ Therefore, through the addition of powder or fiber, the flame retardancy of PBS is leveled up. This implies that the incorporation of powder and fiber into the biodegradable polymers may increase the thermal stabilities of the samples.

SEM analysis

The SEM photograph of Bionolle is shown in Figure 7, whereas the SEM photograph of the untreated fiber-reinforced Bionolle matrix is shown in Figure 8. The compatibility between the untreated fiber and Bionolle

matrix is poor as evidenced by the presence of large space between two components. Furthermore, the compatibility between fiber and Bionolle matrix is improved when the fiber is treated by silane coupling agents as seen in Figures 9 and 10 (SEM photographs of BF10Z6020 and BF10Z6040). This is shown by the densely knitted texture. This implies that the coupling agents play an important role as compatibilizer between the fiber and polymer matrix. The SEM photograph of BP10 is shown in Figure 11. It is found that the homogeneity of the blends is better than those of fiber-containing samples because of the smaller particle size of the powder.

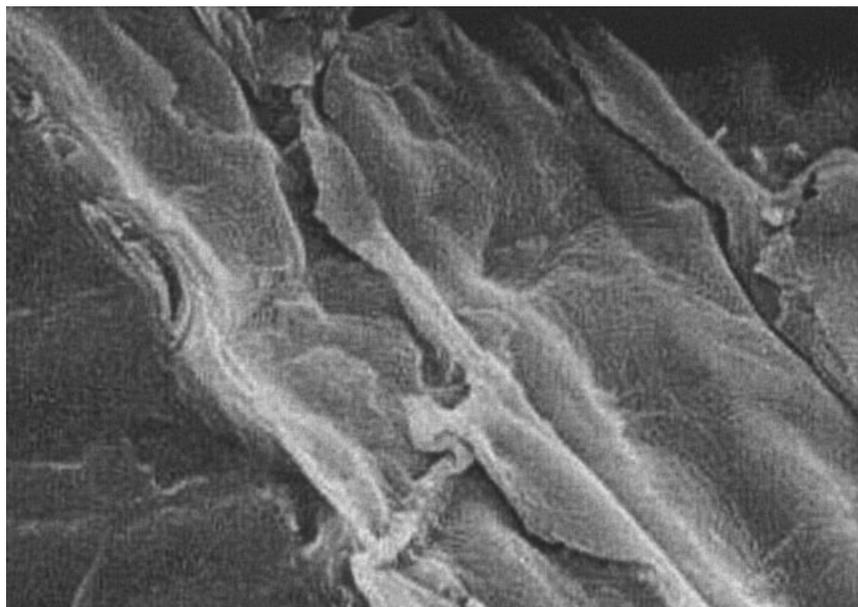


Figure 10 SEM photograph (2000 \times) of BF10Z6040.

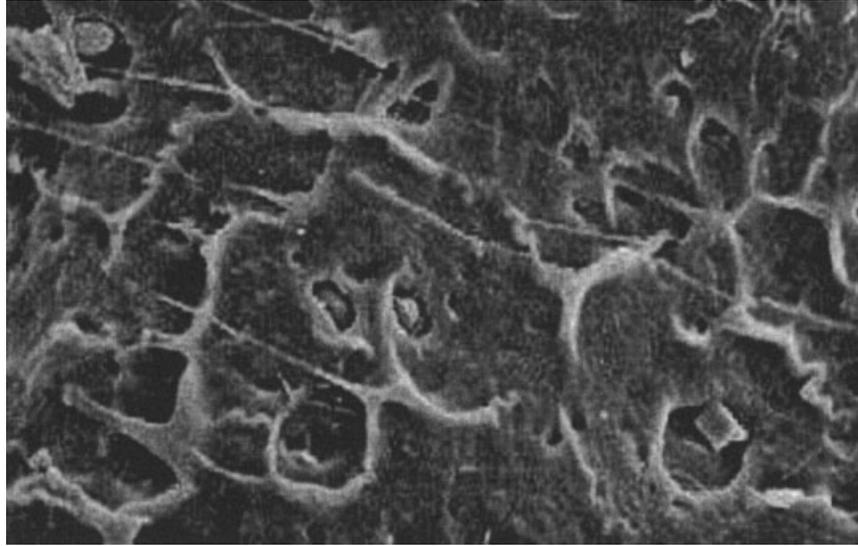


Figure 11 SEM photograph (2000 \times) of BP10.

DMA analysis

As shown in Figure 12, the storage modulus of BP10 is larger than that of Bionolle. However, the storage modulus of BF10 is similar to that of Bionolle. Moreover, the loss modulus of BP10 is larger than that of Bionolle (Fig. 13). However, the loss modulus of BF10 is somewhat smaller than that of Bionolle. These results along with the SEM analysis imply that better homogeneity was obtained for the BP10 sample. Consequently, the BP10 sample exhibited better dynamic mechanical properties. This may be due to the smaller particle size of the powder, leading to the better com-

patibility between the powder and polymer matrix. Better compatibility would bring about better mechanical properties.³¹ As shown in Figures 14 and 15, the storage and loss moduli of BF10Z6040 are larger than those of Bionolle and other fiber-containing samples, BF10 and BF10Z6020. This indicates that the coupling agent Z6040 seems to perform better in improving the compatibility of polymer matrix and the fiber than Z6020. On the other hand, the storage and loss moduli of BP10Z6020 and BP10Z6040 are similar to those of Bionolle despite that the storage and loss moduli of BP10 are larger than those of Bionolle (Figs. 16 and 17).

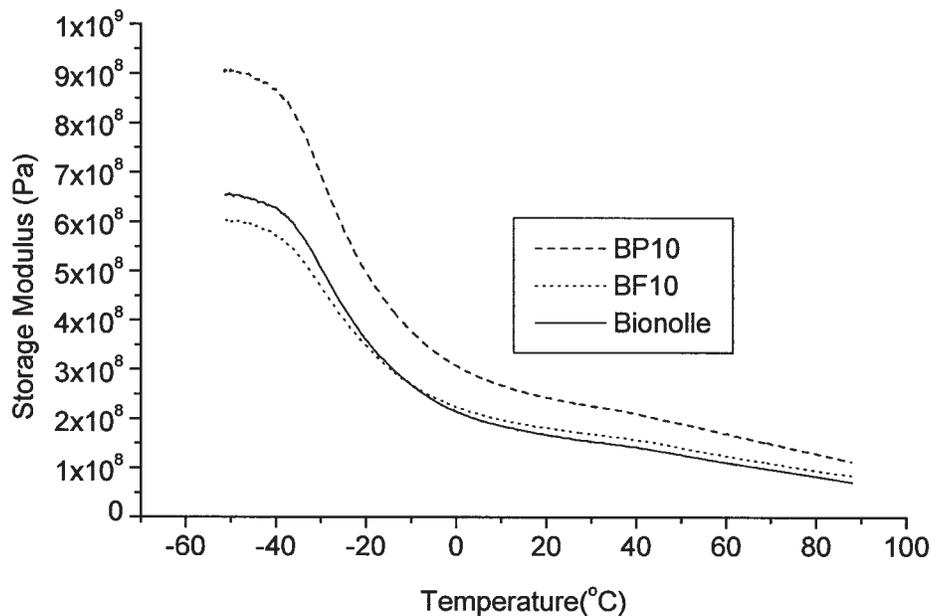


Figure 12 Temperature dependence of the storage moduli for noncoupling agent-treated materials.

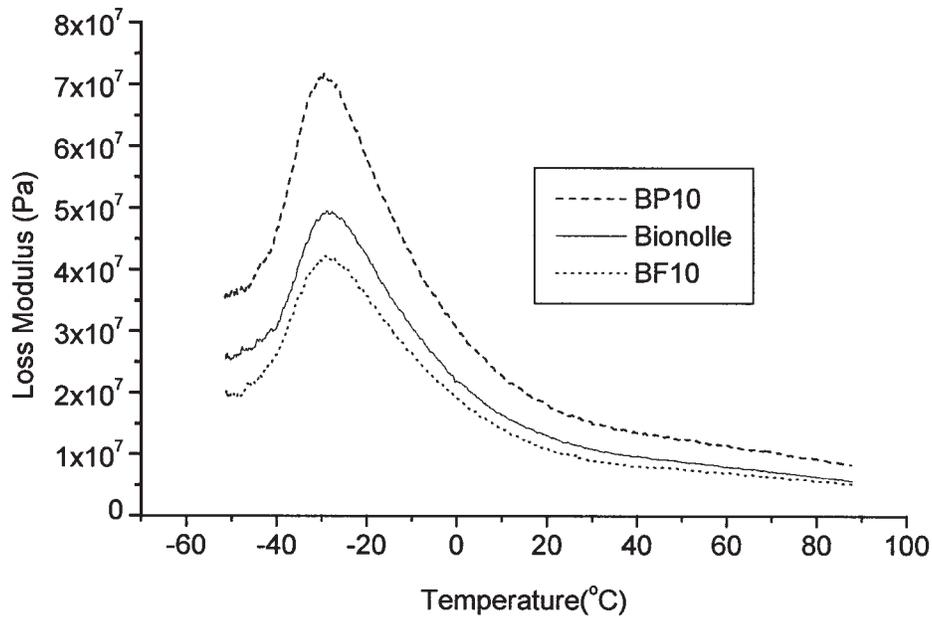


Figure 13 Temperature dependence of the loss moduli for noncoupling agent-treated materials.

This implies that the powder modified with coupling agents was not effective in improving the mechanical properties of the reinforced Bionolles such as BP10Z6020 and BP10Z6040. This is due to that cellulose is the main component of vegetable fibers, whereas the powder is composed of hemicellulose and lignin.³⁸ Cellulose molecules consist of unbranched chains up to 20,000 1,4-linked *b*-D-glucose residues.³⁹ Thus, there are still three hydroxyl groups on glucose rings. This polyhydroxylic nature leads to the high

polarity of cellulose. However, the structural building blocks of lignin are linked by C—C and ether bonds. Units that are trifunctionally linked to adjacent units represent branching sites, which give rise to the network structure characteristic of lignin. Thus lignin consists of rather complex and diverse structures.^{40,41} Moreover, the bulky structure of lignin leads to the smaller reaction ratio with the coupling agents. Consequently, the coupling agents were not effective for the powder modification.

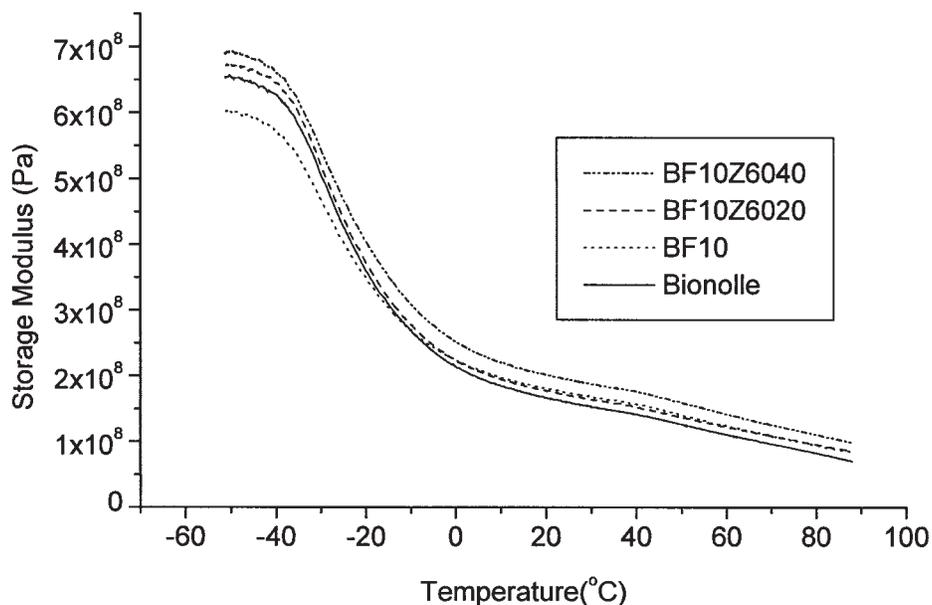


Figure 14 Temperature dependence of the storage moduli for fiber-containing materials.

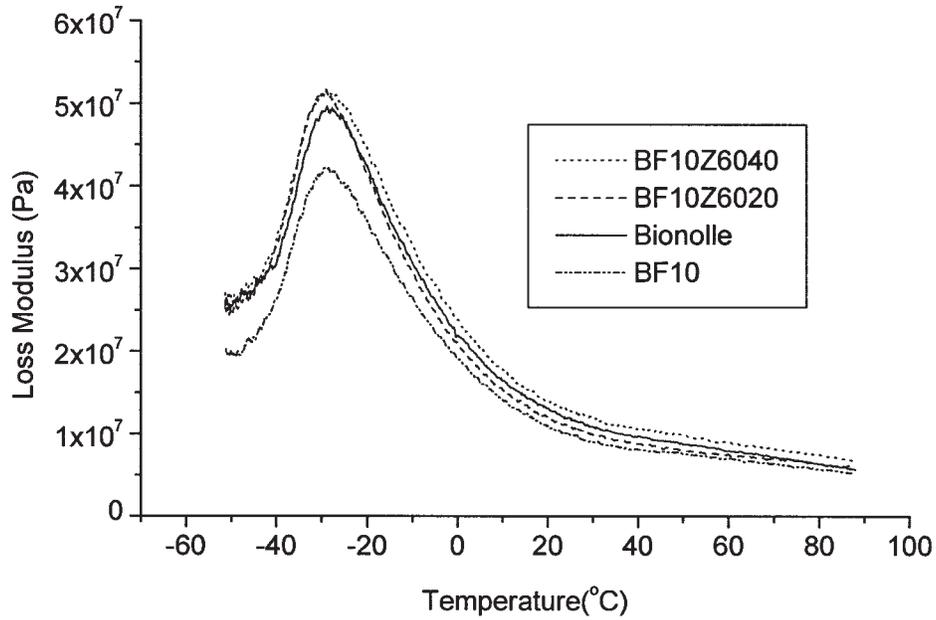


Figure 15 Temperature dependence of the loss moduli for fiber-containing materials.

Adiabatic calorimeter measurement

As shown in Table III, the HOCs of powder and fiber are far smaller than that of Bionolle. Moreover, the HOCs are reduced with the addition of fiber or powder into Bionolle (e.g., BF10, BP10, BP10Z6020, BP10Z6040, BF10Z6020, and BF10Z6040). This implies that the addition of powder and fiber is effective in inhibiting the rise in temperature in burning conditions.

CONCLUSIONS

For the biodegradable plastics (Bionolle), the addition of the fiber or powder obtained from water bamboo husk improves the mechanical and thermal properties of the reinforced materials. Moreover, the addition of powder can enhance the storage modulus and loss modulus of the materials effectively. Because of the innate biodegradability of water bamboo husk, this type of reinforced plastics would

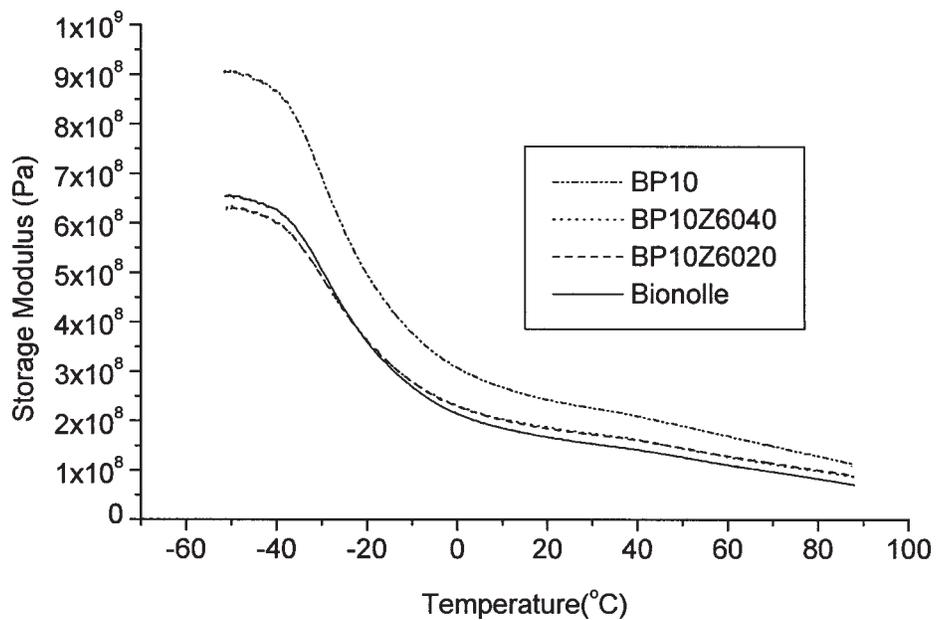


Figure 16 Temperature dependence of the storage moduli for powder-containing materials.

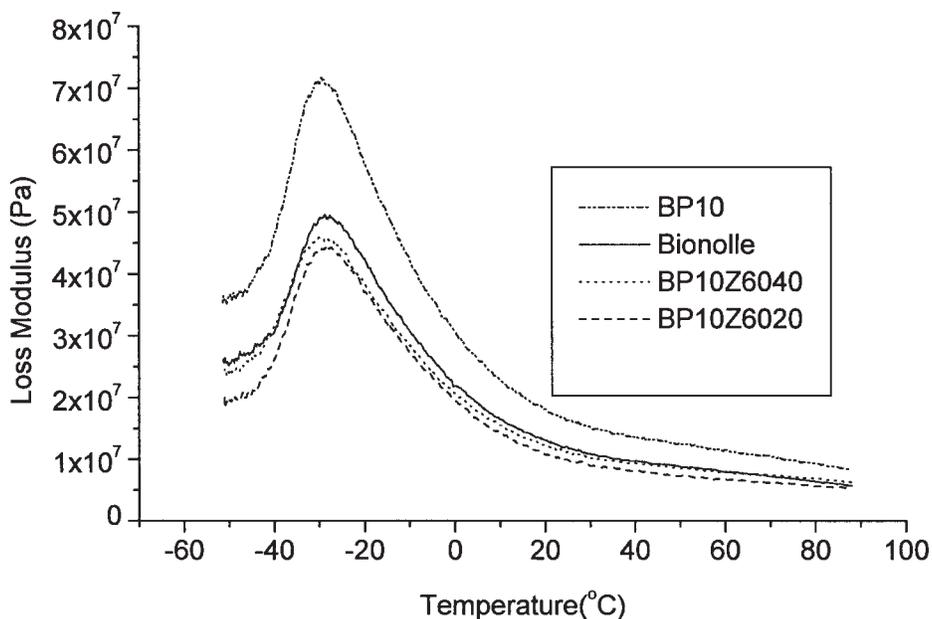


Figure 17 Temperature dependence of the loss moduli for powder-containing materials.

TABLE III
HOC of Samples

Samples	HOC (kJ g ⁻¹)
B	21.90
P	14.36
F	15.69
BP10	21.59
BF10	21.62
BP10Z6020	20.91
BP10Z6040	21.17
BF10Z6020	21.22
BF10Z6040	21.42

be more environmental friendly than the traditional ones. Furthermore, the agricultural wastes could be reduced through the usage as plastic-reinforced additives.

References

- Lin, T. S.; Juang, S. S. *Agricultural Reports of Taichung District Agricultural Improvement Station, Taichung, Taiwan*, 1999, 26, 9.
- Rana, A. K.; Mitra, B. C.; Baberjee, A. N. *J Appl Polym Sci* 1999, 71, 531.
- Avella, M.; Casale, L.; dell'Erba, R.; Martuscelli, E. *Macromol Symp* 1998, 127, 211.
- Nair, K. C. M.; Kumar, R. P.; Thomas, S.; Schit, S. C.; Ramamurthy, K. *Composites: Part A* 2000, 31, 1231.
- Gassan, J.; Gutowski, V. S. *Compos Sci Technol* 2000, 60, 2857.
- Hepworth, D. G.; Vincent, J. F. V.; Jeronimidis, G.; Bruce, D. M. *Composites: Part A* 2000, 31, 599.
- Dash, B. N.; Rana, A. K.; Mishra, H. K.; Nayak, S. K.; Mishra, S. C.; Tripathy, S. S. *Polym Compos* 1999, 20, 62.
- Hill, C. A. S.; Khalil, H. P. S. *J Appl Polym Sci* 2000, 78, 1685.
- Deshpande, A. P.; Rao, M. B.; Rao, C. L. *J Appl Polym Sci* 2000, 76, 83.
- Oksman, K. L.; Berglund, W. L. A. *J Appl Polym Sci* 2002, 84, 2358.
- Thwe, M. M.; Liao, K. *Composites: Part A* 2002, 33, 43.
- Stael, G. C.; Tavares, M. I. B. *Polym Test* 2000, 19, 251.
- Pothan, L. A.; Oommen, Z.; Thomas, S. *Comp Sci Technol* 2003, 63, 283.
- Pothan, L. A.; Thomas, S. *Comp Sci Technol* 2003, 63, 1231.
- Rong, M. Z.; Zhang, M. Q.; Liu, Y.; Yang, G. C.; Zeng, H. M. *Comp Sci Technol* 2001, 61, 1437.
- Iannace, S.; Nocilla, G.; Nicolais, L. *J Appl Polym Sci* 1999, 73, 583.
- Teromoto, N.; Urata, K.; Ozawa, K.; Shibata, M. *Polym Degrad Stab* 2004, 86, 401.
- Shibata, M.; Makino, R.; Yosomiya, R. *Polym Polym Comp* 2001, 9, 333.
- Baiardo, M.; Zini, E.; Scandola, M. *Composites: Part A* 2004, 35, 703.
- Uesaka, T.; Nakane, K.; Maeda, S.; Ogihara, T.; Ogata, N. *Polymer* 2000, 41, 8449.
- Fujimaki, T. *Polym Degrad Stab* 1998, 59, 209.
- Abdelmouleh, A.; Boufi, S.; Salah, A.; Belgacem, M. N.; Gandini, A. *Langmuir* 2002, 18, 3203.
- Wu, H. D.; Chu, P. P.; Ma, C. C. M.; Chang, F. C. *Macromolecules* 1999, 32, 3097.
- Shih, Y. F.; Jeng, R. J. *Polym Int* 2004, 53, 1892.
- Britcher, L.; Kehoe, D.; Matisons, J.; Swincer, G. *Macromolecules* 1995, 28, 3110.
- Pouchert, C. J., Ed.; *The Aldrich Library of Infrared Spectra*, 3rd ed; Aldrich Chemical Co.: Milwaukee, 1981, p 62, 123, 1535.
- Valadez-Gonzalez, A.; Cervantes-Uc, J. M.; Olayo, R.; Herrera-Franco, P. J. *Composites Part B* 1999, 30, 321.
- Wagner, C. D.; Riggs, W. M.; Muilenberg, G. E., Eds.; *Handbook of X-ray Photoelectron Spectroscopy*; PerkinElmer Corporation: Minnesota, 1979.
- Toth, A.; Bertóti, M.; Bánhegyi, G.; Bogнар, A.; Szaplanczay, P. *J Appl Polym Sci* 1994, 52, 1293.

30. Krevelen, D. W. *Polymer* 1975, 16, 615.
31. Shih, Y. F.; Jeng, R. J. *J Appl Polym Sci* 2002, 86, 1904.
32. Banks, M.; Ebdon, J. R.; Johnson, M. *Polymer* 1993, 34, 4547.
33. Wang, C. S.; Shieh, J. Y. *J Appl Polym Sci* 1999, 73, 353.
34. Liu, Y. L. *Polymer* 2001, 42, 3445.
35. Wu, C. S.; Liu, Y. L.; Hsu, K. L. *Polymer* 2003, 44, 565.
36. Shih, Y. F.; Wang, Y. T.; Jeng, R. J.; Wei, K. M. *Polym Degrad Stab* 2004, 86, 339.
37. Pearce, E. M.; Leipins, R. *Environ Health Perspect* 1975, 11, 69.
38. Bledzki, A. K.; Reihmane, S.; Gassan, J. *J Appl Polym Sci* 1996, 59, 1329.
39. French, A. D.; Bertoniere, N. R.; Brown, R. M.; Chanzy, H.; Gray, D.; Hattori, K.; Glasser, W. *Encyclopedia of Polymer Science and Technology: Cellulose*; Wiley: New York, 2003.
40. Lebo, S. E.; Gargulak, J. D.; McNally, T. J. *Encyclopedia of Polymer Science and Technology: Lignin*; Wiley: New York, 2003.
41. Willis, A.; Kellogg, S. T. *Biomass: Part B. Lignin*; Academic Press: San Diego, 1988.